

Article

# Groundwater Isotopes in the Sonoyta River Watershed, USA-Mexico: Implications for Recharge Sources and Management of the Quitobaquito Springs

Hector A. Zamora <sup>1,\*</sup>, Christopher J. Eastoe <sup>1,†</sup>, Benjamin T. Wilder <sup>2</sup>, Jennifer C. McIntosh <sup>3</sup>, Thomas Meixner <sup>3</sup> and Karl W. Flessa <sup>1</sup>

<sup>1</sup> Department of Geosciences, University of Arizona, Tucson, AZ 85721, USA; kflessa@arizona.edu

<sup>2</sup> Desert Laboratory on Tumamoc Hill, University of Arizona, Tucson, AZ 85745, USA; bwilder@arizona.edu

<sup>3</sup> Department of Hydrology and Atmospheric Sciences, University of Arizona, Tucson, AZ 85721, USA; jenmc@arizona.edu (J.C.M.); tmeixner@arizona.edu (T.M.)

\* Correspondence: hzamora@email.arizona.edu

† This author is retired.

Received: 30 September 2020; Accepted: 20 November 2020; Published: 24 November 2020

**Abstract:** Groundwater resources in the southwestern United States are finite and riparian and wetland areas are vulnerable to aquifer overdraft and unregulated groundwater use. Environmental isotopes and water chemistry were used to distinguish water types, recharge mechanisms, and residence time along several reaches of the Sonoyta River and Quitobaquito Springs located near the U.S.-Mexico border. Areas located upgradient from the Sonoyta River, such as the Puerto Blanco Mountains and La Abra Plain, are supported by local recharge which corresponds to water from the largest 30% of rain events mainly occurring during winter. For Quitobaquito Springs, the  $\delta^{18}\text{O}$  and  $\delta^2\text{H}$  values are too low to be derived from local recharge. Stable isotope data and  $\text{Cl}/\text{SO}_4$  mass ratios indicate that the Sonoyta River supplied Quitobaquito Springs through flow along a suggested fault system. Based on these results, Quitobaquito Springs flow could be diminished by any activity resulting in increased groundwater extraction and lowering of water elevations in the Sonoyta River regional aquifer.

**Keywords:** groundwater; springs; environmental isotopes; transboundary watershed; Sonoyta River

---

## 1. Introduction

Alluvial aquifers in the Basin and Range Province in western North America have been extensively studied through the use of environmental isotopes ( $\delta^{18}\text{O}$ ,  $\delta^2\text{H}$ ,  $^3\text{H}$ , and  $^{14}\text{C}$ ) and solute chemistry [1–4]. Waters develop distinctive isotopic and chemical compositions as a result of fractionation resulting from the hydrological, biological, and chemical processes that occur at the surface, and in the vadose and saturated zones of the aquifer systems. This geochemical characterization of waters provides the means to distinguish sources of aquifer recharge, identify preferential flow paths, and estimate groundwater residence time [2–4]. The method is particularly effective in high-relief basins that receive recharge from bounding mountain ranges and from rivers with distant headwaters [2,3], such as the Sonoyta River watershed (Figure 1). Here, in the heart of the Sonoran Desert, along the U.S.-Mexico border, ecological systems and human settlements heavily rely on and compete for water resources that are expected to decline as the climate warms and becomes more arid [5].

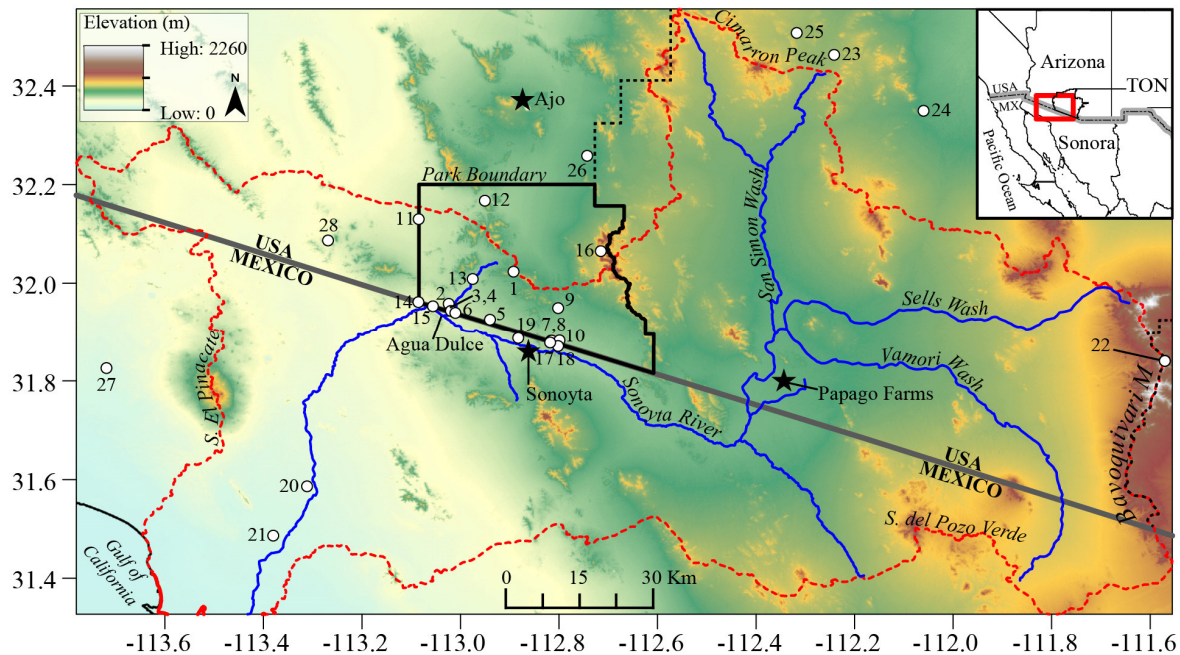


**Figure 1.** Sonoyta River Watershed (delimited by red-dotted line) and major geographical features in the region. Black dashed line shows the limits of the Tohono O'odham Nation (TON). Black bold line shows the limit of the Organ Pipe Cactus National Monument (OPCNM). Sample sites (white circles) are identified by numbers listed in Table 1. Black star symbols show the towns of Ajo, Arizona, Sonoyta, Sonora, and the Papago Farms in the TON.

Perennial surface flow and wetlands (*ciénegas*) occurred along several reaches of the Sonoyta River prior to the 19th century, but have been significantly reduced by the diversion of surface water into irrigated fields [6]. Livestock grazing during the early 20th century severely degraded the river's channel. Over recent decades, the combination of drought conditions with increasing groundwater demand for irrigation and municipal use on both sides of the border has contributed to the decline of water levels in the local alluvial aquifer [7]. Intensive groundwater use started in 1952 and peaked in the 1980s when approximately  $1.32 \times 10^8$  m<sup>3</sup>/year of groundwater were used to irrigate 13,000 ha in the Sonoyta Valley in Mexico, and 2000 ha in the Tohono O'odham Nation [6,8,9]. The volume of water used for irrigation is estimated to have exceeded natural recharge by  $0.97 \times 10^8$  m<sup>3</sup> during this time period [6,9].

Today, surface water resources at Organ Pipe Cactus National Monument (OPCNM, Figure 1) and the lower Sonoyta River are limited to bedrock depressions (*tinajas*) that collect seasonal runoff, springs such as Quitobaquito and Dripping springs (see Figure 2 for location), and few perennial reaches along the river [10,11]. The largest perennial reach occurs 1.6 km south of Quitobaquito Springs (referred to as Quitobaquito below), near the privately-owned Rancho Agua Dulce in Sonora (Figure 2), where granitic bedrock is exposed along a narrow river channel. The perennial reaches of the river are vestiges of a once-intact riparian ecosystem in one of the more arid portions of the Sonoran Desert. The pockets of surface water that persist serve as a refuge to a diversity of native and endemic aquatic vertebrates recognized as endangered or threatened (e.g., Desert Pupfish and the Sonoyta mud turtle; [11]).

The efforts of this study focus around Quitobaquito and the reaches of the Sonoyta River adjacent to OPCNM, and within the Sonoyta Valley and La Abra Plain (Figure 2). Long-term spring flow measurements at Quitobaquito show a reduction in discharge during the last 25 years (Figure 3; [12]). Detailed hydrogeochemical studies that address the origin of groundwater recharge, residence time, and hydrologic connections to surface water are needed to understand the impacts of increased groundwater use and expected intensified drought in aquatic ecosystems. This study uses chemical and isotopic tracers combined with available stratigraphic and piezometric information to assist in these efforts. Our initial hypotheses were that (1) a hydraulic connection exists between the

local aquifer originating in the Puerto Blanco Mountains, previously believed to be the main source of groundwater supporting perennial flow at Quitobaquito, and the regional aquifer of the Sonoyta River and (2) unregulated groundwater use will negatively impact the status of Quitobaquito and the perennial reaches of the Sonoyta River.

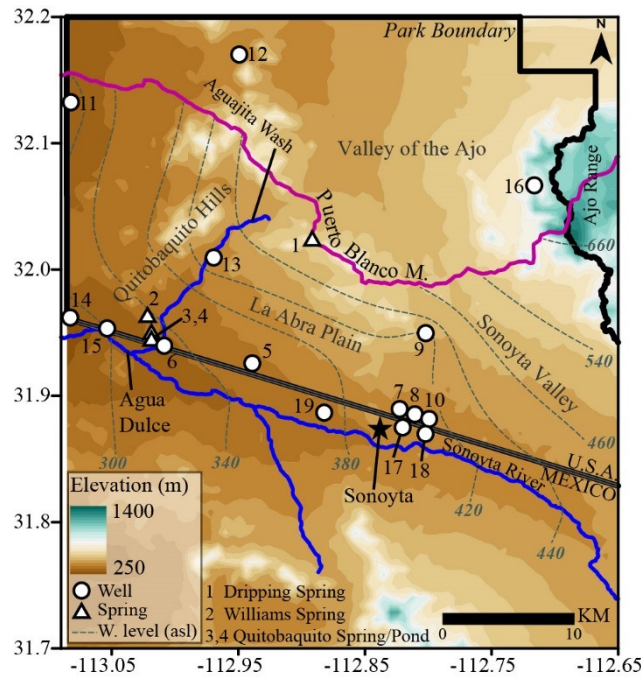


**Figure 2.** Detail of the study area showing the location of water sample collection. Black star symbol shows the location of Sonoyta, Sonora. Pink line shows the watershed boundary, gray-dashed lines show water table elevation in meters above sea level. Water levels on the Mexican side from [13].

To test these hypotheses, we use stable isotopes ( $\delta^{18}\text{O}$  and  $\delta^2\text{H}$ ), radioactive tracers ( $^{14}\text{C}$  and  $^3\text{H}$ ), and major ion chemistry of groundwater, surface water, and precipitation. In southwestern North America, stable isotopes in recharge preserve the signatures related to the altitude and seasonality of precipitation, thus, helping to discriminate between waters of different origin [14–16]. Radioactive tracers can be used to estimate groundwater residence times and identify areas of active recharge [17,18]. Improved knowledge of recharge dynamics and sources of water sustaining riparian areas in the study area can help to manage water resources in this water-stressed region.

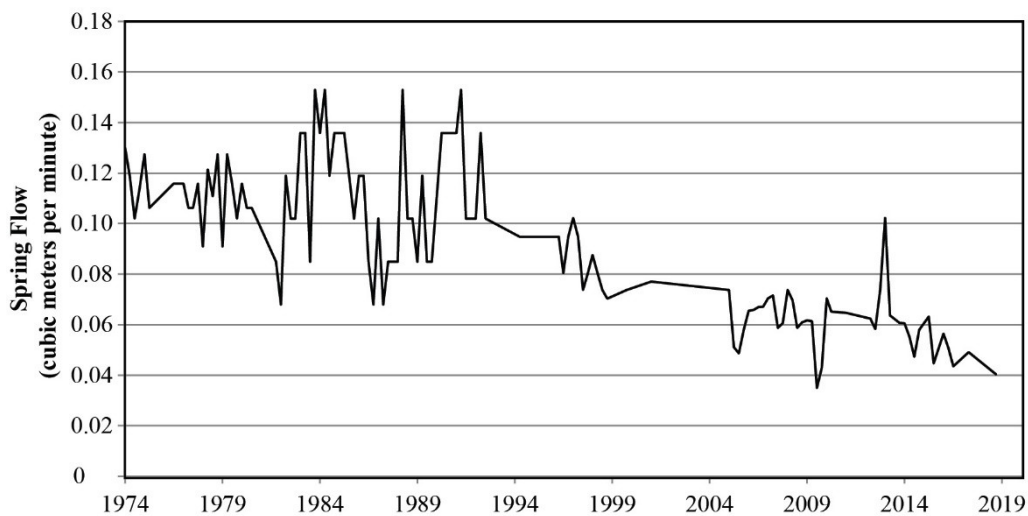


**Figure 3.** Discharge in cubic meters per minute at Quitobaquito from 1973 to 2017 [12].

**Table 1.** Major ion chemistry and environmental isotope data of groundwaters.

Site	Type	Date	T (°C)	pH	E.C. (mS/cm)	Ca <sup>2+</sup> (mg/L)	Mg <sup>2+</sup> (mg/L)	Na <sup>+</sup> (mg/L)	K <sup>+</sup> (mg/L)	Cl <sup>-</sup> (mg/L)	SO <sub>4</sub> <sup>2-</sup> (mg/L)	NO <sub>3</sub> <sup>-</sup> -N (mg/L)	Br <sup>-</sup> (mg/L)	F <sup>-</sup> (mg/L)	HCO <sub>3</sub> <sup>-</sup> (mg/L)	δ <sup>18</sup> O (‰)	δ <sup>2</sup> H (‰)	δ <sup>13</sup> C-DIC (‰)	<sup>3</sup> H (TU)	<sup>14</sup> C (pMC)	Group	
1	Spring	Mar-16	14	6.6	0.28	2	0	69	3	21	29	0.3	0.0	0	195	-5.3	-45	-6.5	1.8	103	C	
		Feb-17	14	8.2	0.24	5	0	76	4	21	26	0		0	207	-4.5	-38				C	
		Mar-11															-5.4	-44				C
		Oct-03	22	6.8	0.33	2	0	64	2	25	36					63						
		May-03		7.2	0.30	1	0	61	2	22	32					53						
		Dec-02	13	7.5	0.41	3	0	79	3	22	25					118						
2	Spring	Dec-76	14	8.3	1.10	33	8	190	4	140	87				307							
		Mar-11															-4.5	-44				C
3	Spring	Feb-17	25	7.6	1.15	38	11	200	5	150	97	3		5	305	-8.4	-59				B	
		Mar-16	28	7.4	1.15	36	12	213	5	170	101	3	0.0	5	480	-8.3	-64	-8.3	1.2	62	B	
4	Spring/Pond	Jul-88	30	7.7	1.15	33	10	190	5	150	87				306							
		Jan-85	25	7.7	1.17	38	11	200	5	160	97				311	-8.3	-61				B	
		Aug-82	28	7.9	1.06	36	10	41	5	150	93				313	-8.4	-63				B	
		Dec-81	25	8.3	1.14	37	11	210	5	150	92				305							
		Nov-76	26	7.9	1.15	36	10	200	5	150	97				311							
5	Well	Jul-83	25	8.4	2.52	30	18	500	3	460	230				432	-7.0	-54	-7.3			A	
		Jan-85	25	7.7	1.19	39	11	210	5	170	98				318	-8.4	-61				B	
6	Well	Jun-83	25	7.7	1.17	40	11	210	9	160	110				337	-8.5	-62	-11.1			B	
		Dec-76	14	8.2	1.30	40	11	210	6	160	110				315							
7	Well	Feb-17	28	8.0	0.83	14	5	160	3	100	68	4		5	195	-8.6	-62				B	
8	Well	Feb-17	26	8.1	0.95	22	8	180	4	140	70	5		5	195	-8.7	-62				B	
		Feb-17	32	7.7	0.78	41	10	103	4	83	52	4		2	198	-8.3	-60				B	
		Mar-16	31	5.8	0.82	25	11	119	4	104	62	5	0.0	2	205	-8.2	-62	-9.6	<0.7	47	B	
		Mar-89	33	8.1	0.86	30	13	120	4	110	64				198							
9	Well	Jul-88	33	7.8	0.82	30	13	120	5	110	60				198							
		Mar-16	28	6.0	0.86	11	5	173	4	106	70	5	0.0	8	284	-8.7	-64	-7.8	<0.5	21	B	
10	Well	Mar-16	38	6.8	4.25	129	7	578	18	868	372	0	2.6	3	118	-7.9	-62	-4.8	<0.5	24	B	
11	Well	Mar-16				84	13	13	3	5	2	0	0.0	0	450	-7.3	-53	-9.0			A	
		Jan-85	16	7.3	0.57	89	12	12	2	6	15				349	-7.5	-52				A	
12	Well	Mar-16	23	7.0	0.70	84	16	54	3	12	2	0	0.0	0	452	-5.9	-44	-3.0	2.6	107		
		Jan-83	25	8.0	0.45	60	12	39	1	7	18				322	-7.5	-53				A	
13	Well	Mar-16	30	7.3	2.05	81	24	438	16	517	148	2	1.8	4	678	-8.0	-61	-2.0	<0.5	73	B	
		Jul-83	31	7.5	1.85	48	10	330	7	280	200				340	-8.0	-61	-9.9			B	
14	Well	Jul-83	24	7.9	2.35	29	10	540	5	350	240				650	-8.1	-64	-7.8			B	
15	Well	Mar-16	21	6.9	0.83	75	17	110	2	104	59	1	0.0	1	455	-7.8	-56	-12.2	0.8	99	A	
16	Well	Apr-16	29	7.2	1.47	39	15	288	6	265	191	6	1.1	5	279	-8.6	-63	-7.6	<0.7	49	B	
17	Well	Apr-16	28	7.5	1.16	28	11	226	4	190	127	5	0.9	6	257	-8.7	-64	-7.5	<0.8		B	

19	Well	Apr-16	24	7.1	1.76	46	12	372	5	265	189	3	1.1	0	643	-8.0	-60	-8.2	<0.7	80	B
20	Well	Apr-16	32	8.0	1.59	15	4	363	5	385	146	0	1.3	0	232	-7.8	-60	-5.5	<1.0	27	
21	Well	Apr-16	31	7.9	1.93	23	16	409	5	473	164	2	1.7	0	438	-7.6	-59	-5.3	<0.5	16	
22	Well	Jun-81	24	7.3	0.58	72	17	30	1	15	66				268	-8.6	-61				B
23	Well	Jan-78	25	8.0	0.58	5	4	114		44	48				165						
		Jan-81	25	8.2	0.58	9	4	110	2	44	40				207	-7.3	-58				A
24	Well	Sep-78		8.4		23	15	109	3	15	61				250						
		Apr-81		8.0	0.81	30	20	120	2	34	100				305	-7.0	-53				A
25	Well	Mar-78	31	7.7	0.53	24	16	61		31	23				222						
		Apr-81			0.53	26	15	60	5	34	22				220	-7.2	-54				A
26	Well	Feb-16		7.8	0.9	27	5	137	5	124	114	4			127	-8.0	-59				B
27	Well	Oct-16		7.6	0.5	17	4	90	4	12	15	5	0.0		348	-7.6	-51		<0.4		A
28	Well	Feb-17	27	7.7	0.549	45	7.4	60	1.9	31	17				268	-7.5	-52				A

Note:  $\delta^{18}\text{O}$  and  $\delta^2\text{H}$  relative to V-SMOW (‰),  $\delta^{13}\text{C-DIC}$  relative to V-PDB (‰).

## 2. Materials and Methods

### 2.1. Study Area

#### 2.1.1. Location

The Sonoita River watershed is located in the Basin and Range Province (Figure 1). It is a transboundary watershed in southern Arizona, United States, and northern Sonora, Mexico, that covers an area of 12,618 km<sup>2</sup> [19]. Major watercourses within the watershed include the Sonoita River originating near the Pozo Verde Mountains in Mexico, and the Vamori, Sells, and San Simon washes draining the Tohono O'odham Nation west of the Baboquivari Mountains and south of Cimarron Peak. The drainage network converges south of the international border, 40 km east of the town of Sonoita, Mexico. From here, the Sonoita River continues parallel to the border, just south of OPCNM, through irrigated lands in Mexico, then turns southwards near the Sierra El Pinacate and infrequently reaches the Gulf of California in the vicinity of Puerto Peñasco.

#### 2.1.2. Climate and Isotopes

Climate is arid to semiarid and precipitation follows a bimodal pattern. Summer precipitation (June–early September) consists of localized, intense, convective precipitation generated during the North American Monsoon from water sources in the tropical eastern Pacific Ocean and the Gulf of California, and accounts for about half of the annual precipitation [20,21]. Winter precipitation consists of widespread and long-lived frontal systems generated in temperate regions of the eastern Pacific [21–23]. Weather stations maintained by the U.S. National Park Service (NPS) staff at OPCNM show that total annual rainfall increases with elevation [24]. The Sonoita Valley, located 400 m above sea level (masl), receives 180 mm/year of rainfall. Ajo Peak, the highest point within OPCNM at 1465 masl, receives ~300 mm/year of rainfall. The highest elevations of the watershed occur at the crest of the Baboquivari Mountains at about 2300 masl. Precipitation data are available at the Kitt Peak National Observatory, 2096 masl, where the annual average is about 560 mm [25]. Average air temperature ranges between 13.1 and 32.6 °C at the lower elevations, and 5 and 21 °C at the higher elevations.

Studies in the Tucson Basin (180 km east of the study area) established that summer and winter precipitation have distinctly different amount-weighted mean values of  $\delta^{18}\text{O}$  and  $\delta^2\text{H}$  reflecting seasonal changes in condensation temperature and moisture source [21,26,27]. An isotope altitude effect is also well-established in the Tucson Basin where lapse-rates of 1.6‰ per 1000 m for  $\delta^{18}\text{O}$ , and 11‰ per 1000 m for  $\delta^2\text{H}$  have been measured [27]. Such distinctions, extrapolated to surrounding basins with few or no isotope data for precipitation, provide evidence of the sources and seasonality of recharge in the region [14,28]. On the basis of isotope evidence, recharge in southern Arizona originates mainly as precipitation from the wettest (30%) months, when sufficient water is present, and conditions are optimal for recharge [14,29].

#### 2.1.3. Geology, Hydrogeology, and Hydrogeochemistry

The Basin-and-Range Province of western North America is characterized by horst and graben physiography consisting of long, narrow mountain ranges separated by alluvium-filled valleys supporting regional groundwater aquifer systems. The geology and hydrogeology of the OPCNM, including the Sonoita Valley, La Abra Plain, and surrounding areas, have been described in previous studies [30–32]. Principal geological units are shown in Figure 4. The study area is bounded to the north and northwest by mountain ranges consisting of Mesozoic igneous and metamorphic rocks exposed by late Cretaceous thrust faulting and tectonic sliding (e.g., Quitobaquito Hills, Puerto Blanco Mountains; [30]). Granite gneiss, schist, granite, and metasedimentary rocks are the main lithological components [31]. To the northeast, the study area is bounded by igneous rocks of late Cretaceous and Tertiary age, include andesite, rhyolite, latite, and granodiorite complexes in the Ajo Range [33].

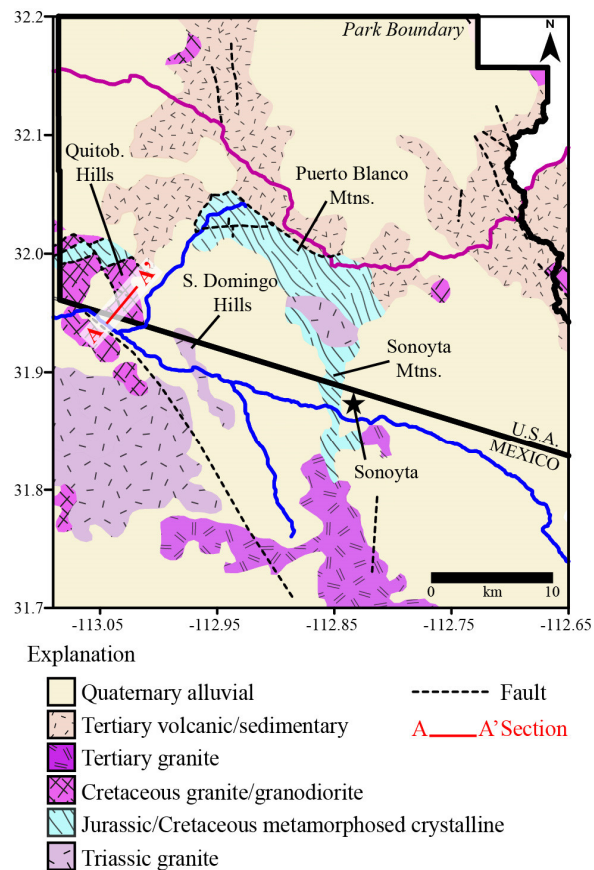


**Figure 4.** Geology of study area. Pink line shows the watershed boundary. Black star symbol shows the location of Sonoyta, Sonora. Map includes data from [34] in the U.S., and from [35] in Mexico.

Basin-fill consists of mainly unconsolidated to weakly consolidated gravels, sands, and silts that overlie pediments on lower slopes, occurring as a set of overlapping and interconnected lenses of alluvium and slope wash adjacent to range fronts [34]. These basin-fill deposits extend outwards from the range fronts as alluvial plains sloping down towards the Sonoyta River Valley where their depths may exceed 300 m. Stream channels have been cut into the less-permeable basin-fill. These deposits are left behind by ephemeral streams (e.g., Aguajita Wash, Figure 2) that originate in the nearby mountains and merge with the Sonoyta River.

Most irrigation wells are drilled in the basin-fill, but groundwater also occurs in stream-channel deposits and fractured granitic rocks on the southwest side of the Quitobaquito Hills where a series of fault-controlled springs are found (e.g., Quitobaquito; Figure 5, [34]). Reported hydraulic conductivities range between 110 and 11,000 m/year for alluvial basin-fill in southern Arizona [36]. Hydraulic conductivity is low in volcanic, crystalline, and metamorphic rocks, but can be enhanced if weathering and/or fracturing is extensive [37]. Estimated hydraulic conductivities range between 0.7 and 5.10 m/year for fractured igneous and metamorphic rocks in southern Arizona [38].

Recharge in the regional Sonoyta River basin is likely influenced by mountain system recharge occurring at the basin margins as in other semi-arid basins in southern Arizona [28]. Mountain system recharge includes all water sourced in the mountain block entering a basin-fill aquifer, known as mountain-front recharge, and subsurface inflow of groundwater coming directly from the mountain block to lowland aquifers, known as mountain-block recharge [39]. Other important contributions in this setting include flood-driven recharge in the ephemeral stream network and irrigation reflux along the Sonoyta River. Diffuse recharge, defined as the direct infiltration of rainwater and subsequent percolation to the water table, is assumed to be negligible.

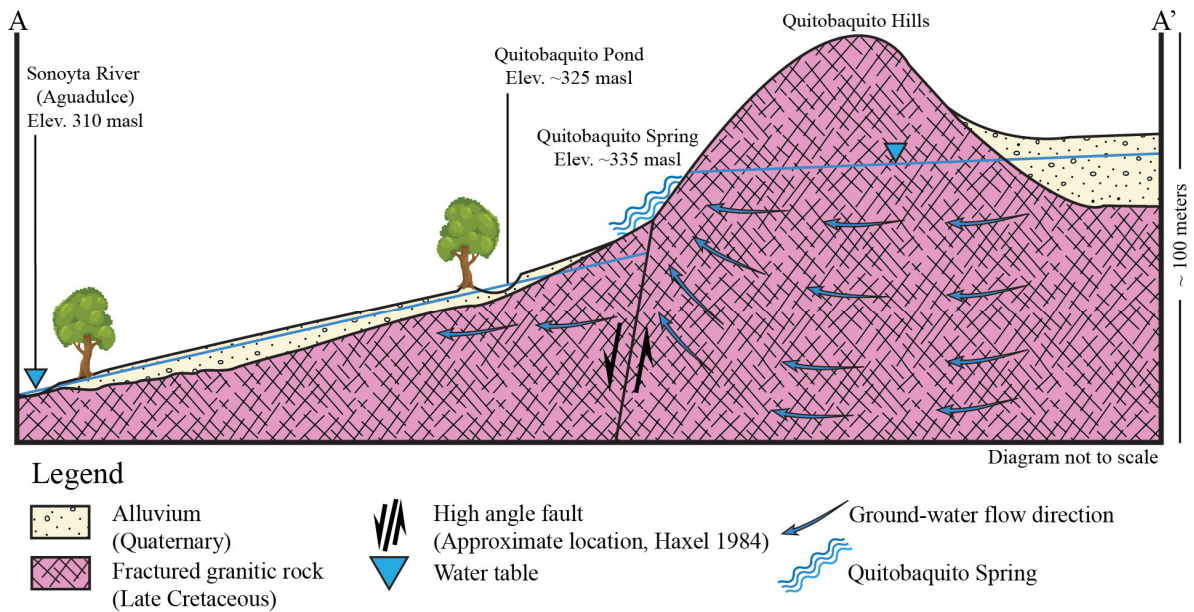


**Figure 5.** Cross-section of the Quitobaquito Springs area. See Figure 4 for cross-section trace location. Modified from [34].

The chemical character of groundwaters depends on the location. Recharge areas tend to be dominated by Ca-HCO<sub>3</sub> water types and low concentrations of total dissolved solids. Down gradient areas in alluvial basins tend to be dominated by Na-HCO<sub>3</sub>-Cl water types (see Figure 6; [40]). SO<sub>4</sub><sup>2-</sup> to Cl<sup>-</sup> ratios were used in the nearby San Pedro River, in southeastern Arizona, to differentiate basin groundwater from monsoon flood recharge sustaining intermittent streamflow [41].

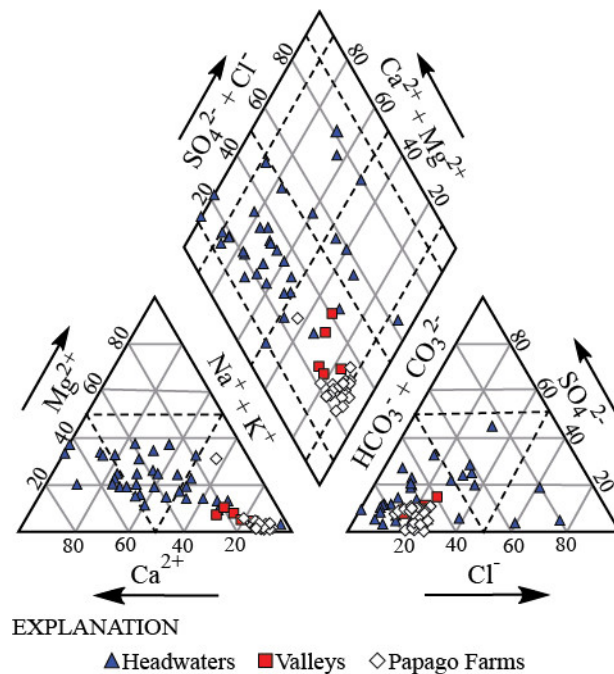


**Figure 6.** Piper Diagram showing data for groundwater samples along the Sonoyta River course. “Headwater” samples were collected near the Baboquivari Mountains, “Valleys” samples were collected along the floodplains downstream, and “Papago Farms” samples were collected within the irrigated fields of the Tohono O’odham Nation (see Figure 1 for location). Data from Water Quality Portal [42].



## 2.2. Data Collection and Analysis

Groundwater samples were collected from shallow monitoring wells and agricultural wells, which range in depth from 3 to 300 m. No surface water samples were collected from the Sonoyta River, which was dry during the period of the study. Water supplied in the past by the river is represented by shallow groundwater from the river flood plain. Except for site 13, wells were purged of three well volumes, or bailed, unless they were in continuous use. For this reason, the ( $\delta^{18}\text{O}$ ,  $\delta^2\text{H}$ ) values for site 13 collected in March 2016 are left out of the discussion. Spring samples were collected in March 2016 from Dripping Springs (site 1), located near the top of the Puerto Blanco Mountains at an elevation of ~650 masl, and Quitobaquito, located at an elevation of ~335 masl, and within 200 m north of the international border (Figure 2, sites 3 and 4). Rainfall samples were collected between 2015 and 2017 from rain gauges within OPCNM (adjacent to sites 1, 3, 9, 12, and 16) prepared with a thin layer of mineral oil to prevent evaporation. Aggregate rainwater samples were recovered during several visits to the study area in late October and late March of the respective years.

For groundwater and surface water samples, pH, temperature, and electrical conductivity were measured in the field using a YSI 556 Multiparameter System sonde calibrated with standard pH and conductivity buffers. Samples for measurement of ions and alkalinity were filtered into 30 mL HDPE bottles using 0.45- $\mu\text{m}$  nylon membranes. Samples for analysis of cations were preserved by the addition of two drops of optima-grade  $\text{HNO}_3$ . Samples for measurement of stable O, H, and C isotopes were filtered as above and kept stored in 20 mL glass containers. For age tracers ( $^3\text{H}$  and  $^{14}\text{C}$ ), we stored unfiltered 1-L water samples in rinsed HDPE and amber-glass bottles, respectively. All samples were stored on ice in the field and refrigerated at 4 °C in the laboratory.

Stable O and H isotopes were measured on a gas-source isotope ratio (Finnigan Delta-S) mass spectrometer with automated  $\text{CO}_2$  equilibration and Cr reduction attachments at the University of Arizona's Environmental Isotope Laboratory. Values for stable O and H are reported in delta notation relative to VSMOW (Vienna standard mean ocean water) with standardization based on international reference materials SLAP (standard light Antarctic precipitation) and VSMOW. Precision is 0.9‰ or better for  $\delta^2\text{H}$  and 0.08‰ or better for  $\delta^{18}\text{O}$ . Values for stable C were measured on a Gasbench automated sample attached to a continuous-flow mass spectrometer (Thermo-Finnigan Delta Plus XL, Bremen, Germany). Samples were reacted with phosphoric acid at room temperature in He-flushed Exetainer vials. Tritium ( $^3\text{H}$ ) was measured by liquid scintillation spectrophotometry on electrolytically enriched samples mixed 1:1 with Ultimagold Low-Level Tritium cocktail. The detection limit was 0.5 TU for 1500 min of counting using a Wallac Oy Quantulus 1220 Spectrophotometer (Turku, Finland) at the University of Arizona. Calibration for  $^3\text{H}$  was relative to NIST SRM 4361, and results are presented as tritium units (TU). For radiocarbon ( $^{14}\text{C}$ ), carbon was extracted as  $\text{CO}_2$  from 1-L unfiltered water samples and reduced to graphite. The product was measured by accelerator mass spectrometry on a National Electrostatics Pelletron AMS at the NSF-Arizona AMS facility. Calibration for  $^{14}\text{C}$  was relative to IAEA Oxalic Acids I and II, and results are presented as percent modern carbon (pMC). Anion (excluding  $\text{HCO}_3^-$ ) and cation concentrations were obtained using a Dionex DX-600 Ion Chromatography system, and an Elan DRC-II Inductively Coupled Plasma–Mass Spectrometer (precision  $\pm 2$ ), respectively, at the University of Arizona Laboratory for Emerging Contaminants (ALEC). Alkalinity was obtained using the Gran-Alkalinity method [43], and the results were used in a PHREEQC speciation model to estimate  $\text{HCO}_3^-$  in mg/L [44].

New data and previously published isotope and ion chemistry for the Sonoyta River basin from the Water Quality Portal [42] are presented in Table 1. Water Quality Portal data, which includes data from the U.S. Geological Survey's National Water Information System (NWIS) and U.S. Environmental Protection Agency's (EPA) Storage and Retrieval Data Warehouse (STORET), has been published in previous studies [9,13,34]. Table 1 includes all individual values for sites with multiple data (see Table S1 for locations).

Rainfall data collected in the study area are insufficient to provide valid estimates of the long term mean  $\delta^{18}\text{O}$  and  $\delta^2\text{H}$  values. Due to this shortfall, we combine our results with stable isotope data obtained from the United States Network for Isotopes (USNIP; [45]) station at OPCNM's visitor

center (510 masl) as previously published by Zamora et al., 2019 (Figure 7A; [46]). The seasonal, amount-weighted means (Figure 7B) were calculated using  $\delta^{18}\text{O}$  and  $\delta^2\text{H}$  data for individual rainfall events (Figure 7A). Stable isotope data from *tinaja* samples collected by NPS during March and April of 2011 are used to estimate the evaporation trend in the area (Figure 8). Throughout the text, we use the terms “locally sourced” groundwater or “local recharge” to refer to groundwaters recharged near OPCNM, or at similar elevations in the lower parts of the basin, in contrast to “high elevation” recharge which refers to water sourced at the headwaters or margins of the Sonoyta River basin.

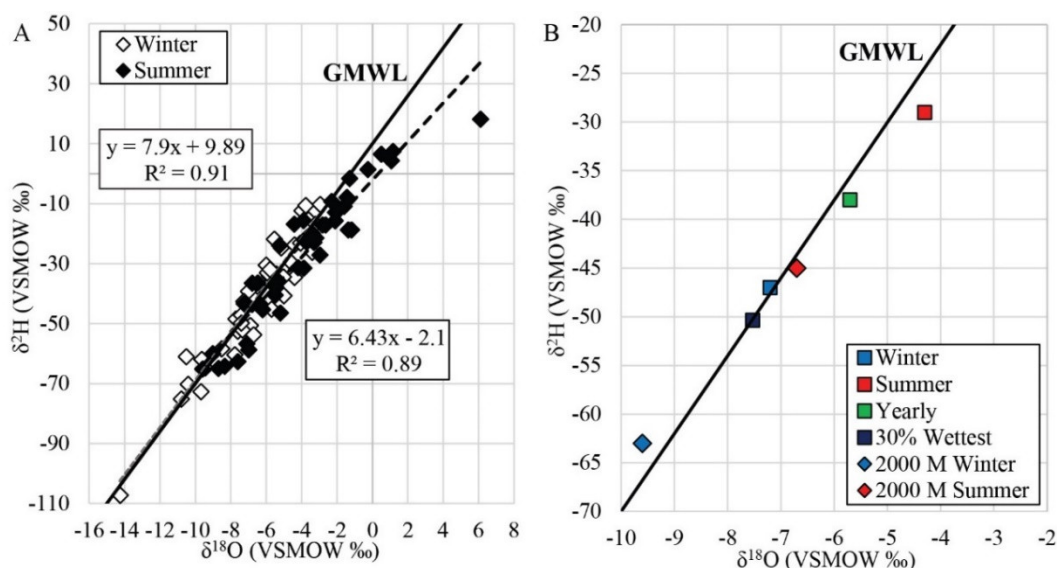


**Figure 7.** (A).  $\delta^{18}\text{O}$  and  $\delta^2\text{H}$  values for individual precipitation events collected within Organ Pipe Cactus National Monument between 1990 and 2016 at an elevation of ~510 masl (from [46]). (B). Amount-weighted mean ( $\delta^{18}\text{O}$ ,  $\delta^2\text{H}$ ) values for winter (November to April), summer (May to October), all events (labeled “Yearly”), and the 30% most intense events (including summer and winter) from data in (A). “2000 M Winter” and “2000 M Summer” was calculated using the mean isotopic altitude effects in Tucson, Arizona (1.6‰ per 1000 m for  $\delta^{18}\text{O}$  and 11‰ per 1000 m for  $\delta^2\text{H}$ ) [27] and the elevation difference between OPCNM’s visitor center and the Baboquivari Mountains (~1490 m).

### 3. Results

#### 3.1. Rainfall

Data for rainfall collected during the winter months (November to April) closely match the Global Meteoric Water Line (GMWL; [47]) and follow a trend with a slope of 7.9 and y-intercept of 9.89 ( $R^2 = 0.91$ , Figure 7A; [46]). Data for summer rainfall (May to October) plot slightly below the GMWL, and follow a trend with a slope of 6.43 and y-intercept of  $-2.11$  ( $R^2 = 0.89$ , Figure 7A; [46]). The amount-weighted mean ( $\delta^{18}\text{O}$ ,  $\delta^2\text{H}$ ) values are  $-4.3\text{‰}$  and  $-29\text{‰}$  for summer precipitation,  $-7.2\text{‰}$  and  $-47\text{‰}$  for winter rainfall,  $-5.7\text{‰}$  and  $-38\text{‰}$  for all rainfall events, and  $-7.5\text{‰}$  and  $-50\text{‰}$  for the 30% most intense events (Figure 7B). If we apply the mean isotopic altitude effects of the Tucson Basin (1.6‰ per 1000 m for  $\delta^{18}\text{O}$  and 11‰ per 1000 m for  $\delta^2\text{H}$ ) to the OPCNM means (assuming an elevation difference of 1490 m between the rain gauge location at OPCNM’s visitor center and the Baboquivari Mountains), we estimate ( $\delta^{18}\text{O}$ ,  $\delta^2\text{H}$ ) values of  $-9.6\text{‰}$  and  $-63\text{‰}$  for average winter precipitation, and  $-6.7\text{‰}$  and  $-45\text{‰}$  for average summer precipitation at the highest elevations of the Sonoyta River basin (2000 masl, Figure 7B). For comparison, the average ( $\delta^{18}\text{O}$ ,  $\delta^2\text{H}$ ) values at an elevation of 2000 masl for the Catalina Mountains, near Tucson, Arizona are  $-10.5\text{‰}$  and  $-66\text{‰}$  for winter, and  $-8.0\text{‰}$  and  $-53\text{‰}$  for summer [27].

3.2. Tinajas

Tinajas had  $\delta^{18}\text{O}$  values ranging between  $-4.9$  and  $+7.7\text{‰}$ , and  $\delta^2\text{H}$  values ranging between  $-30$  and  $+10\text{‰}$ . The data plot on an evaporation line of slope 3.16 ( $R^2 = 0.82$ , Figure 8).

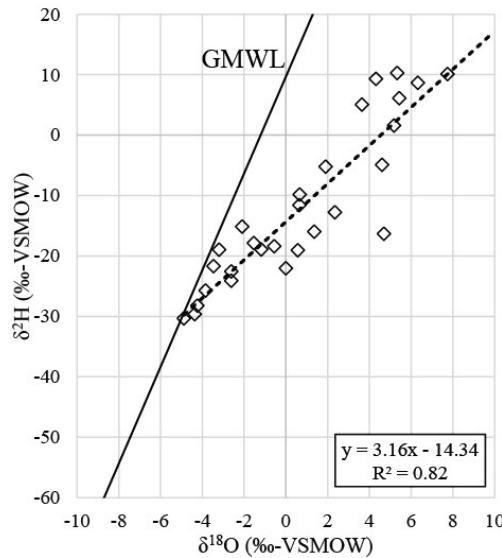


Figure 8.  $\delta^{18}\text{O}$  and  $\delta^2\text{H}$  values for water samples collected by the NPS from tinajas during March and April 2011 [48].

3.3. Groundwater

Groundwaters in the Sonoyta River basin transition from  $\text{Ca-HCO}_3$  type near the headwaters, adjacent to the Baboquivari Mountains, to  $\text{Na-HCO}_3$  type upgradient of the international border. Degradation of water quality is associated with the presence of lakebed-clay deposits near Papago Farms (see Figure 1; [9]). Within the study area, only groundwaters from sites 12 (Valley of the Ajo) and 13 (in La Abra plain) are  $\text{Ca-HCO}_3$  type, and the rest are  $\text{Na-HCO}_3\text{-Cl}$  and  $\text{Na-Cl}$  types (Figure 9). Other ions including  $\text{F}^-$ ,  $\text{NO}_3^-$ , and  $\text{Br}^-$  are reported in Table 1. These ions are not further discussed but are presented here as a reference for future studies.

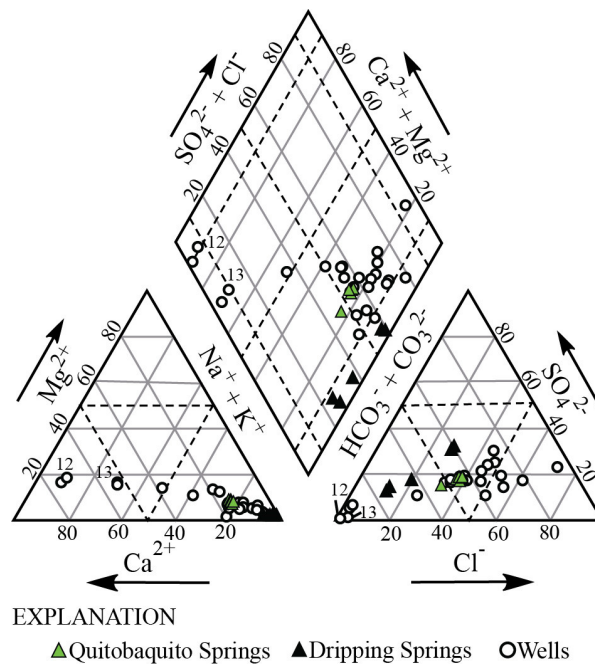
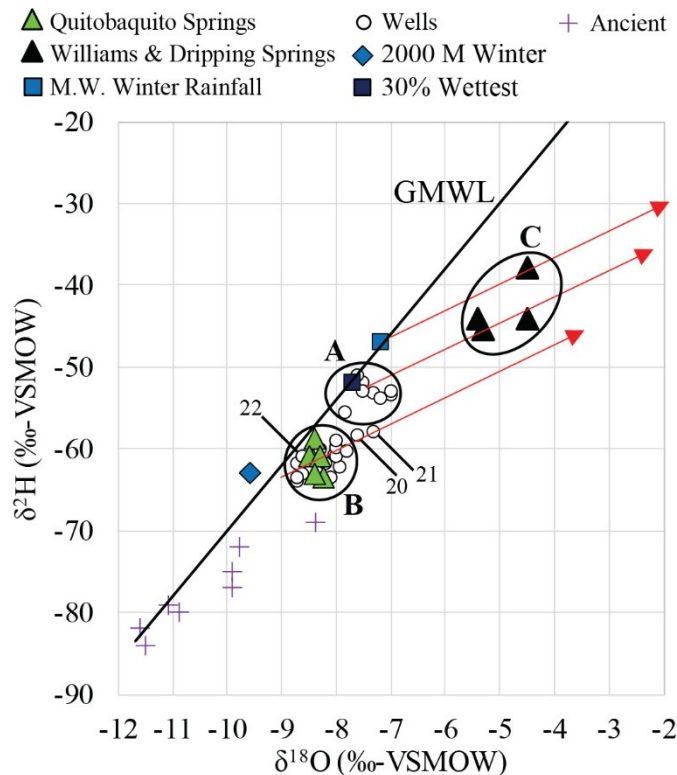


Figure 9. Piper Diagram showing major ion chemistry data for springs and well water samples in the study area.

Three groups of water isotope data are present in Figure 10 (Table 2). For samples in Group A,  $\delta^{18}\text{O}$  values range between  $-7.0$  and  $-7.8\text{‰}$ , and  $\delta^2\text{H}$  values range between  $-51$  and  $-58\text{‰}$ . This group includes samples from sites 5, 12, 13, 16, 23, 24, 25, 27, and 28. For samples in Group B,  $\delta^{18}\text{O}$  values range between  $-7.9$  and  $-8.7\text{‰}$ , and  $\delta^2\text{H}$  values range between  $-59$  and  $-64\text{‰}$ . This group includes samples from sites 3, 4, 6, 7, 8, 9, 10, 11, 14, 15, 17, 18, 19, 22, 26, and includes the data for the Quitobaquito system (discussed below). Samples from the lowest reaches of the river (sites 20 and 21, Figure 1) plot next to group B, but more evaporated. Levels of  $^3\text{H}$  and  $^{14}\text{C}$ , are lower near the Sonoyta River than at sites near the Puerto Blanco Mountains (except for site 11, 25 pMC; Figure 11). Site 13, located along the Aguajita Wash had the highest values for both radioisotopes (2.6 TU and 107 pMC; Figure 11).



**Figure 10.**  $\delta^{18}\text{O}$  and  $\delta^2\text{H}$  values for mean rainfall (winter, and other values shown in Figure 7B), springs, and wells. Red arrows show the expected evaporation trend in the area with a slope of 3.16 obtained from Figure 8. Quitobaquito samples (from spring and pond) are shown by green-filled triangles in Group B. Ancient water samples (uncorrected pMC < 10) in southern Arizona from [2]. Wells east (upstream) of Quitobaquito along the Sonoyta River floodplain (7, 8, 10, 17, 18, 19) have ( $\delta^{18}\text{O}$ ,  $\delta^2\text{H}$ ) ranges between  $-8.7$  and  $-8.0\text{‰}$  and  $-64.1$  and  $-60\text{‰}$  respectively.

**Table 2.** Summary of maximum and minimum ( $\delta^{18}\text{O}$ ,  $\delta^2\text{H}$ ) values for groups A, B, and C in Figure 10.

Group	$\delta^{18}\text{O}$ - Max	$\delta^{18}\text{O}$ - Min	$\delta^2\text{H}$ - Max	$\delta^2\text{H}$ - Min	Sites
A	-7.0	-7.8	-51	-58	5, 12, 13, 16, 23, 24, 25, 27, 28
B	-7.9	-8.7	-59	-64	3, 4, 6, 7, 8, 9, 10, 11, 14, 15, 17, 18, 19, 22, 26
C	-4.5	-5.4	-38	-45	1, 2

### 3.4. Springs

Dripping Springs (site 1) samples tend to have  $\text{Na-HCO}_3$  chemistry, while Quitobaquito samples are  $\text{Na-HCO}_3\text{-Cl}$  water types (Figure 9). In terms of stable isotopes, there is a clear difference between the two systems. For Dripping Springs,  $\delta^{18}\text{O}$  values range between  $-4.5$  and  $-5.4\text{‰}$ , and  $\delta^2\text{H}$  values range between  $-38$  and  $-45\text{‰}$ . These values comprise Group C in Figure 10 (Table 2). For

Quitobaquito,  $\delta^{18}\text{O}$  values range between  $-8.3$  and  $-8.5\text{‰}$ , and  $\delta^2\text{H}$  values range between  $-59$  and  $-64\text{‰}$  (Figure 10; Group B). Williams Spring (site 2) is adjacent to Quitobaquito, and plots within Group C. The samples from both sites plot below the GMWL (Figure 10). A Dripping Spring sample had a  $^3\text{H}$  value of 1.8 TU, and  $^{14}\text{C}$  value of 103 pMC. For Quitobaquito, the  $^3\text{H}$  value was 1.2 TU, and the  $^{14}\text{C}$  value was 62 pMC (Figure 11).

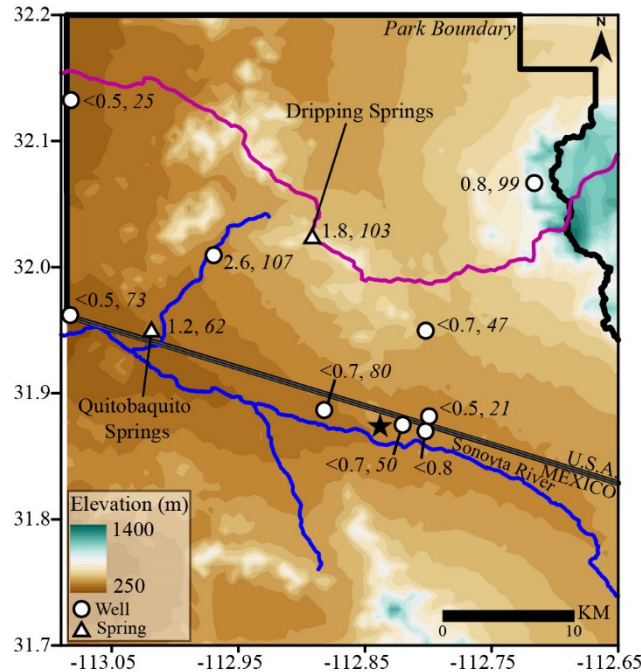


**Figure 11.** Tritium (TU), and Carbon-14 data (pMC) for groundwater samples in the study area. Pink line shows the watershed boundary. Black star symbol shows location of the town of Sonoyta, Sonora. See Figure 1 for sample site identification.

### 3.5. Summary of Geographic Distribution

The groups defined by isotope chemistry have a specific geographic distribution. Group A occurs away from the main stem of the Sonoyta River mainly along small tributaries draining low-elevation mountain ranges near or within OPCNM. Group B is found close to the Sonoyta River. Group C is limited to the vicinity of the Puerto Blanco Mountains with the exception of the Williams Spring sample (Figures 2 and 10).

## 4. Discussion

### 4.1. Recharge Sources

Well sites 12, 28, and 27 are located away from the Sonoyta River (Figure 1). The ( $\delta^{18}\text{O}$ ,  $\delta^2\text{H}$ ) values for these three sites plot along the GMWL, and represent local recharge (around  $-7.5\text{‰}$  and  $-52\text{‰}$ , Figure 10). Similar values have been observed in the lower Gila River basin, adjacent to the study area [49]. For areas located upgradient from the Sonoyta River, such as the Puerto Blanco Mountains and La Abra Plain, the local recharge is the only possibility. Group A in Figure 10 occurs within this area and corresponds closely to local recharge. Local recharge also corresponds to water from the largest 30% of rain events which tend to occur during the winter months ( $-7.5\text{‰}$  and  $-50\text{‰}$ ; Figure 10). Group C must also be locally sourced and appears to be the evaporated equivalent of Group A, or in one case the evaporated equivalent of mean winter precipitation.

Groundwaters in Group B have a distinct isotopic composition, indicating a different source than group A and C waters. Group B groundwaters occur in the Sonoyta River flood plain, including sites ~20 km upstream of Quitobaquito, where they cannot originate from the spring area. Such water is best explained as originating in the Baboquivari Mountains because its isotope composition

resembles that found at site 22 (Figure 10). The ( $\delta^{18}\text{O}$ ,  $\delta^2\text{H}$ ) values ( $-8.6\text{‰}$  and  $-61\text{‰}$ ) of site 22 are (1) close to the value estimated for mean winter precipitation at 2000 masl in the Baboquivari Mountains; and (2) in agreement with other localities in southern Arizona where groundwater may originate as precipitation from  $>1500$  masl, such as the town of Patagonia where ( $\delta^{18}\text{O}$ ,  $\delta^2\text{H}$ ) values range between  $-10.5\text{‰}$  and  $-8.2\text{‰}$  for oxygen and  $-7.3\text{‰}$  and  $-58\text{‰}$  for hydrogen (average  $-8.7\text{‰}$  and  $-62\text{‰}$ ; [50]).

Group B water also occurs at Quitobaquito, where its origin is not so clear, but the possibilities include: (a) the Sonoyta River, if a plausible flow path can be identified (discussed further below), (b) hurricane rain, but this is unlikely to affect only the spring [51], and/or (c) Late Pleistocene precipitation which had lower ( $\delta^{18}\text{O}$ ,  $\delta^2\text{H}$ ) values in most or all of North America [52]. In southern Arizona, the shift from modern to lower ( $\delta^{18}\text{O}$ ,  $\delta^2\text{H}$ ) values occurred at 13–14 ka [53], corresponding to about 18 pMC. Paleobotanical remains from packrat middens in the area dating back to 22,000–11,000 years B.P. suggest a precipitation decrease ranging from 16% to 70% from the wetter Pleistocene to Holocene conditions (depending on the elevation), with the Pleistocene dominated by winter rain, and having temperatures at least 5 °C lower than today [54–57].

The  $^{14}\text{C}$  content at Quitobaquito, 62 pMC, could be explained as an approximate 1:1 mixing between modern local recharge (100 pMC) and water recharged 13,500 years ago (18 pMC), assuming no addition of dead radiocarbon from carbonate dissolution which would lower the pMC. If the same mixing ratio is used on  $\delta^{18}\text{O}$  data, the local recharge value ( $-7.5\text{‰}$ ) and the Quitobaquito value ( $-8.4\text{‰}$ ) can be used to calculate the value for Pleistocene water which would have been  $\sim -9.4\text{‰}$ , and consistent with the regional 2‰ shift [48,49]. Such value ( $\sim -9.4\text{‰}$ ) is within the range of ancient waters (uncorrected pMC < 10) found in southern Arizona [2] which are shown in Figure 10. The fault zone near Quitobaquito contains local recharge represented by the Williams Spring sample with a temperature of 14 °C (see Table 1). This, and the 1.2 TU at Quitobaquito, are consistent with the mixing of waters in the fault zone.

The volume of groundwater stored in the basin-fill for the local flow system around the fault zone is estimated to range between  $2.11 \times 10^7 \text{ m}^3$  and  $3.66 \times 10^7 \text{ m}^3$  [34]. If we assume that this volume is discharged in its entirety through the Quitobaquito system at a rate of  $1.7 \times 10^2 \text{ m}^3/\text{day}$  [34], this would yield a residence time ranging between 340 and 590 years. This calculation suggests that the fault zone cannot accommodate enough paleowater to sustain the spring for 13,000 years, or that a larger volume of water is stored in the fractured granite.

A hydraulic connection between the local groundwater at Quitobaquito and the regional groundwater beneath the Sonoyta River is plausible [34]. The fault zone from which the springs discharge ( $\sim 335$  masl) may extend southeast to the Sonoyta River on the indication of vegetation anomalies observed in satellite images, and the presence of a former perennial reach south of the Santo Domingo Hills [2]. This hypothetical fault would closely follow the 335 m contour in Figure 12 (red-dotted line).

A southeast continuation of the fault could intersect the river where the 335 m topographic contour (red-dotted line in Figure 12) crosses the channel. When the river had perennial water in the past, perhaps during cooler and wetter times or prior to major irrigation development, it would have been capable of supplying water to the suggested fault zone, and into Quitobaquito. Upward flow in the fault zone at Quitobaquito may be driven by regional hydraulic gradients. The  $\text{SO}_4^{2-}$  and  $\text{Cl}^-$  concentrations at Quitobaquito are higher than those of local recharge and more similar to those of Sonoyta River waters (Figure 13). Similarly, the mass ratio of  $\text{Cl}/\text{SO}_4$  at Quitobaquito and Sonoyta River water plot close to each other suggesting a common origin (Figure 14).

In summary, there are two possible explanations for the origin of water at Quitobaquito and observed decreasing flows, (1) paleo recharge, although estimated groundwater storage volume is too small to accommodate Pleistocene-aged waters, and (2) Sonoyta River water supplying water through the suggested fault zone, which deserves further study. If paleo recharge mixed with local recharge is the source, current drought conditions may be affecting the head in the fault zone due to lowered local recharge fluxes. If water is derived from the Sonoyta River or the alluvial aquifer, present groundwater extraction has probably already impacted the water supply to the spring. The

latter explanation seems to be more plausible based on the ionic mass ratio of  $\text{Cl}^-$  and  $\text{SO}_4^{2-}$ , which suggests Quitobaquito is sourced from the Sonoyta River.

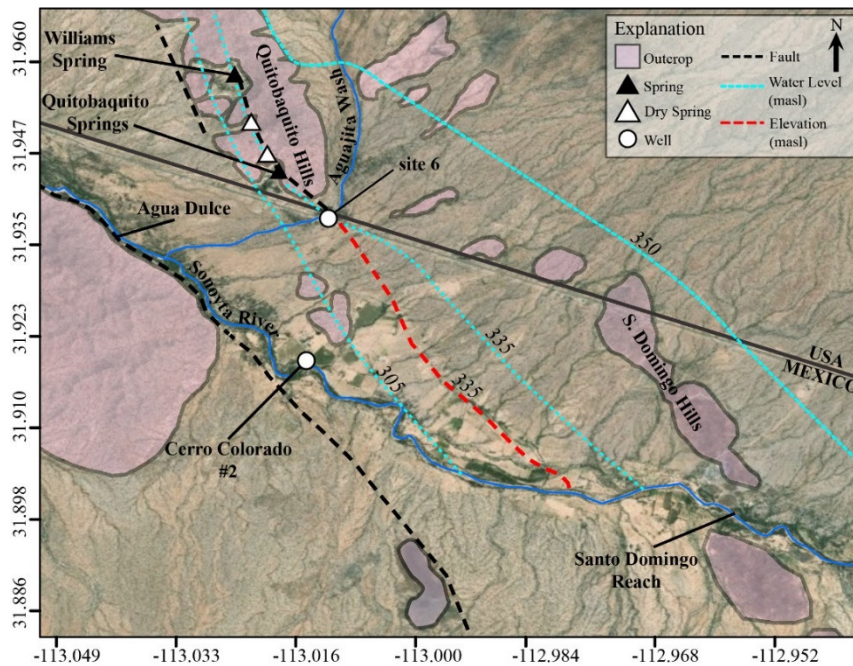


**Figure 12.** Quitobaquito Springs area. Red dotted line shows the 335 m elevation contour and a hypothetical fault, related to the fault system that created Quitobaquito, extending into Mexico.

4.2. Other Data

Samples 20 and 21 plot outside groups A and B (Figure 10). However, these two samples are slightly different in terms of  $\text{Cl}^-$  and  $\text{SO}_4^{2-}$ , and  $^{14}\text{C}$ . The concentrations for both anions are higher in these two samples than in most of the samples in groups A and B (Figure 13) and  $^{14}\text{C}$  pMC are the lowest among all samples (16 and 27 pMC). At a first glance, these samples can be interpreted as analogous to Group B but evaporated prior to recharge. Both samples are located in the southernmost locations along the Sonoyta River and were obtained from wells near irrigated lands (Figure 1). The high degree of evaporation could reflect irrigation reflux into the aquifer, although the low  $^3\text{H}$  and  $^{14}\text{C}$  pMC values do not suggest recent exposure to the atmosphere.

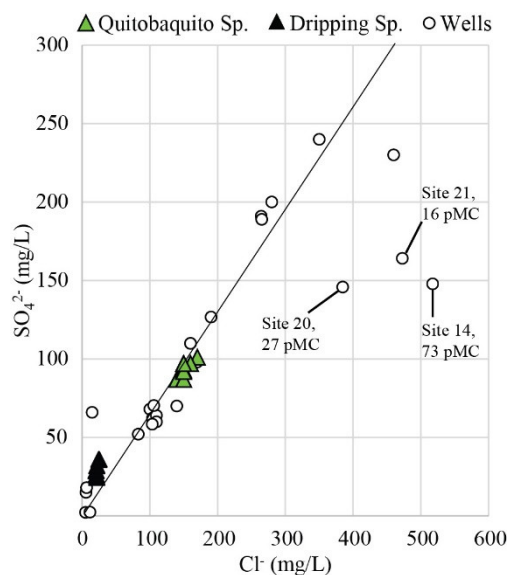


**Figure 13.**  $\text{Cl}^-$  vs  $\text{SO}_4^{2-}$  values for spring and well samples. Diagonal line shows hypothetical evaporation line.

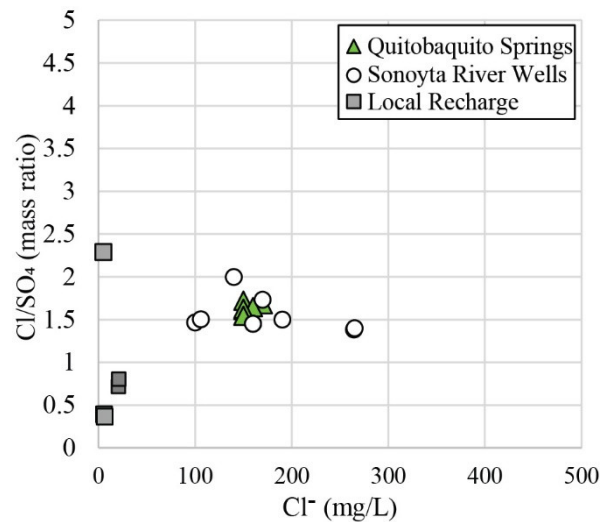


**Figure 14.** Cl/SO<sub>4</sub> vs Cl<sup>-</sup> concentrations for local recharge (sites 1, 12, 13, 27, and 28), Quitobaquito (sites 3, and 4), and Sonoyta River wells upstream of Quitobaquito (sites 7, 8, 10, 17, 18, and 19).

## 5. Conclusions

Areas located upgradient from the Sonoyta River, such as the Puerto Blanco Mountains and La Abra Plain, which include Group A and Group C groundwater (Figure 10), are supported by local recharge. Local recharge corresponds to water from the largest 30% of rain events, dominated by winter events (−7.5‰ and 50‰). Groundwaters in the Sonoyta River floodplain (Group B, Figure 10), ~20 km upstream of Quitobaquito, originate in the Baboquivari Mountains where recharge occurs at a higher elevation. For Quitobaquito, the δ<sup>18</sup>O and δ<sup>2</sup>H values are too low to be derived from local recharge. Two possible explanations for the origin of water at Quitobaquito include (1) a mix of modern recharge and Pleistocene-aged groundwater and (2) Sonoyta River water supplying water through a suggested fault system connecting the spring to the alluvial aquifer beneath the river. The estimated groundwater storage volume around Quitobaquito is too small to accommodate Pleistocene-aged waters, thus it is more likely the spring is fed by the Sonoyta River or its alluvial aquifer, as seen in the similar Cl/SO<sub>4</sub> mass ratios and the δ<sup>18</sup>O and δ<sup>2</sup>H values.

The conclusions here presented have important implications for the management of water resources within OPCNM and the lower Sonoyta River. To further test the nature of the hydrologic connection between the Sonoyta River and alluvial aquifer and Quitobaquito, more detailed field investigations along the fault zones near Quitobaquito are needed. The strategic installation of monitoring wells near Quitobaquito could provide valuable information regarding the subsurface geology, groundwater levels, aquifer properties, and access for the sampling and analysis of stable isotopes and solute chemistry in water. Seismic refraction and magnetic methods around Quitobaquito, including reaches of the Sonoyta River in Mexico along OPCNM, could be useful to find the extension of known faults and outline the existence of others. Detailed studies of isotopes and solute chemistry in groundwater are also needed within the Tohono O’odham Nation. These studies could help identify other potential water sources that could play an important role in the Quitobaquito system. Updated water level information along the Mexican side of the border is vital. This information can be synthesized in a calibrated groundwater model that could help to (1) better understand the present hydrologic conditions of the Quitobaquito and Sonoyta River systems, (2) identify sensitive areas that require further study, (3) re-create past conditions, and/or (4) simulate the spatial and temporal response of the local aquifer under different scenarios of groundwater extraction.

Future climate scenarios predict declines in recharge of varying magnitudes in the southwest region of the United States [58]. Binational collaboration between government agencies in the U.S. and Mexico is critically needed. Further hydrogeological studies are imperative to conserve water



resources for the sustainable development of human communities, and the preservation of natural resources in this arid part of the Sonoran Desert.

**Supplementary Materials:** The following are available online at [www.mdpi.com/2073-4441/12/12/3307/s1](http://www.mdpi.com/2073-4441/12/12/3307/s1), Table S1: Sampling sites locations.

**Author Contributions:** Conceptualization, H.A.Z., C.J.E., and T.M.; methodology, H.A.Z., C.J.E., and J.C.M.; validation, H.A.Z., C.J.E., and J.C.M.; formal analysis, H.A.Z., C.J.E., and J.C.M.; investigation, H.A.Z.; resources, K.W.F., B.T.W., C.J.E., T.M.; writing—original draft preparation, H.A.Z.; writing—review and editing, C.J.E., B.T.W., K.W.F., T.M., J.C.M.; visualization, H.A.Z., C.J.E.; supervision, K.W.F., J.C.M., and T.M.; project administration, H.A.Z., and K.W.F.; funding acquisition, B.T.W., C.J.E., and T.M. All authors have read and agreed to the published version of the manuscript.

**Funding:** This research was funded in part by the National Park Service Southwest Border Resource Protection Program (SBRPP, Grant number P16AC00045), and the University of Arizona Graduate and Professional Student Council Grant.

**Acknowledgments:** The authors express their gratitude to Peter Holm, Charles Connor, Rick Morawe, and Ami Pate at Organ Pipe Cactus National Monument, Colleen Filippone, and Douglas Towne for their resource support, logistics, and assistance during fieldwork.

**Conflicts of Interest:** The authors declare no conflict of interest.

## References

- Smith, G.I.; Friedman, I.; Veronda, G.; Johnson, C.A. Stable isotope compositions of waters in the Great Basin, United States, 3, Comparison of groundwaters with modern precipitation. *J. Geophys. Res.* **2002**, *107*, 4402, doi:10.1029/2001JD000567.
- Eastoe, C.J.; Wright, W. Hydrology of Mountain Blocks in Arizona and New Mexico as Revealed by Isotopes in Groundwater and Precipitation. *Geosciences* **2019**, *9*, 461, doi:10.3390/geosciences9110461.
- Eastoe, C.J.; Rodney, R. Isotopes as Tracers of Water Origin in and Near a Regional Carbonate Aquifer: The Southern Sacramento Mountains, New Mexico. *Water* **2014**, *6*, 301–323, doi:10.3390/w6020301.
- Hopkins, C.B.; McIntosh, J.C.; Eastoe, C.; Dickinson, J.E.; Meixner, T. Evaluation of the importance of clay confining units on groundwater flow in alluvial basins using solute and isotope tracers: The case of Middle San Pedro Basin in southeastern Arizona (USA). *Hydrogeol. J.* **2014**, *22*, 829–849, doi:10.1007/s10040-013-1030-0.
- Barnett, T. Human-induced changes in the hydrology of the western United States. *Science* **2008**, *319*, 1080–1083, doi:10.1126/science.1152538.
- Rosen, P.; Melendez, C.; Riedle, J.; Pate, A.F. Ecology and Conservation in the Sonoyta Valley, Arizona and Sonora. In *Southwestern Desert Resources*; Halvorson, W., Schwalbe, C., Van Ripper, C., III, Eds.; University of Arizona Press: Tucson, AZ, USA, 2010; pp. 143–160.
- Minckley, C.; Izaguirre Pompa, I.D.; Timmons, R.; Caldwell, D.L.; Rosen, P. Native Aquatic Vertebrates: Conservation and Management in the Río Sonoyta Basin, Sonora, Mexico. In *Proceedings of the Merging Science and Management in a Rapidly Changing World: Biodiversity and Management of the Madrean Archipelago*, Tucson, AZ, USA, 1–5 May 2012; Gottfried, G.J., Folliot, P.F., Gebow, B.S., Eskew, L.G., Collins, L.C., Eds.; U.S. Department of Agriculture, Forest Service: Fort Collins, CO, USA, 2013; RMRS-P-67.
- Murguía, M.D.L. El agua en la Reserva de la Biosfera el Pinacate y Gran Desierto de Altar, Sonora, Mexico. *Nat. Res. J.* **2000**, *40*, 411–434.
- Hollet, K. Geohydrology and Water Resources of the Papago Farms-Great Plain Area, Papago Indian Reservation, Arizona, and the Upper Rio Sonoyta Area, Sonora, Mexico. In *U.S. Geological Survey Water-Supply Paper*; U.S. Geological Survey: Reston, VA, USA, 1985; Volume 2258, pp. 1–51.
- Hendrickson, D.; Varela-Romero, A. Conservation status of desert pupfish, *Cyprinodon macularius*, in Mexico and Arizona. *Copeia* **1989**, *1989*, 479–483, doi:10.2307/1445447.
- Miller, R.; Fuiman, L. Description and conservation status of *Cyprinodon macularius eremus*, a new subspecies of pupfish from Organ Pipe Cactus National Monument, Arizona. *Copeia* **1987**, *1987*, 593–609, doi:10.2307/1445652.
- Holm, P. (National Park Service, Tucson, AZ, USA). Personal communication, 2017.

13. Goodman, B. Hydrogeology of the Quitobaquito Springs Area, La Abra Plain, and the Rio Sonoyta Valley, Organ Pipe Cactus National Monument, Arizona and Sonora, Mexico. Master's Thesis, University of Arizona, Tucson, AZ, USA, 1992.
14. Eastoe, C.; Towne, D. Regional zonation of groundwater recharge mechanisms in alluvial basins of Arizona: Interpretation of isotope mapping. *J. Geochem. Explor.* **2018**, *194*, 134–145, doi:10.1016/j.gexplo.2018.07.013.
15. Winograd, I.; Riggs, A.; Coplen, T. The relative contribution of summer and cool-season precipitation to groundwater recharge, Spring Mountains, Nevada, USA. *Hydrogeol. J.* **1998**, *6*, 77–93, doi:10.1007/s100400050135.
16. Cunningham, E.; Long, A.; Eastoe, C.; Bassett, R. Migration of recharge waters downgradient from the Santa Catalina Mountains into the Tucson basin aquifer, Arizona, USA. *Hydrogeol. J.* **1998**, *6*, 94–103, doi:10.1007/s100400050136.
17. Eastoe, C.; Gu, A.; Long, A. The origins, ages and flow paths of groundwater in Tucson Basin: Results of a study of multiple isotope systems. In *Groundwater Recharge in a Desert Environment: The Southwestern United States*; Hogan, J.F., Phillips, F.M., Scanlon, B.R., Eds.; Am. Geophys Union: Washington, DC, USA, 2004; pp. 217–234, doi:10.1029/009WSA12.
18. Sanford, W.; Plummer, L.; McAda, D.; Bexfield, L. Hydrochemical tracers in the Middle Rio Grande Basin, USA: 2. Calibration of a groundwater-flow model. *Hydrogeol. J.* **2004**, *12*, 389–407, doi:10.1007/s10040-004-0326-4.
19. Harshbarger & Associates, Inc. *Overview Report of Groundwater Basins along International Boundary Arizona, U.S. and Sonora, Mexico*; The U.S. Section of the International Boundary and Water Commission: El Paso, TX, USA, 1979; Volume Pr-236-79-1, pp. 1–124.
20. Hereford, R. *Entrenchment and Widening of the Upper San Pedro River, Arizona*; Geological Society of America: Boulder, CO, USA, 1993; pp. 1–282, doi:10.1130/SPE282-p1.
21. Wright, W.; Long, A.; Comrie, A.; Leavitt, S.; Cavazos, T.; Eastoe, C. Monsoonal moisture sources revealed using temperature, precipitation, and precipitation stable isotope timeseries. *Geophys. Res. Lett.* **2001**, *28*, 787–790, doi:10.1029/2000GL012094.
22. Sellers, W.; Hill, R. *Arizona Climate 1931–1972*; The University of Arizona Press: Tucson, AZ, USA, 1974; pp. 1–616.
23. The Western Regional Climate Center: Climate of Arizona. Available online: <https://wrcc.dri.edu/narratives/ARIZONA.htm> (accessed on 20 December 2016).
24. Conner, C. (National Park Service, Tucson, AZ, USA). Personal communication, 2017.
25. The Western Regional Climate Center. Climatological Data Summaries. Available online: <https://wrcc.dri.edu/xummary/Climsmaz.html> (accessed on 15 September 2017).
26. Eastoe, C.; Dettman, D.L. Isotope amount effects in hydrologic and climate reconstructions of monsoon climates: Implications of some long-term data sets for precipitation. *Chem. Geol.* **2016**, *430*, 78–89, doi:10.1016/j.chemgeo.2016.03.022.
27. Wright, W.  $\delta D$  and  $\delta^{18}O$  in Mixed Conifer Systems in the U.S. Southwest: The Potential of  $\delta^{18}O$  in *Pinus ponderosa* Tree Rings as a Natural Environmental Recorder. Ph.D. Thesis, University of Arizona, Tucson, AZ, USA, 2001.
28. Wahi, A.; Hogan, J.; Ekwurzel, B.; Baillie, M.; Eastoe, C. Geochemical Quantification of Semiarid Mountain Recharge. *Ground Water* **2008**, *46*, 414–425, doi:10.1111/j.1745-6584.2007.00413.x.
29. Jasechko, S.; Taylor, R. Intensive rainfall recharges tropical groundwaters. *Environ. Res. Lett.* **2015**, *10*, 124015, doi:10.1088/1748-9326/10/12/124015.
30. Haxel, G.; Tosdal, R.; May, D.; Wright, J. Latest Cretaceous and early Tertiary orogenesis in south-central Arizona—Thrust faulting, regional metamorphism, and granitic plutonism. *Geol. Soc. Am.* **1984**, *94*, 631–653.
31. Gray, F.; Miller, R.; Grubensky, M.; Tosdal, R.; Haxel, G.; Peterson, D.; May, D.J.; Silver, L.T. *Geologic Map of the Ajo and Lukeville 1° by 2° Quadrangle, Southwest Arizona*; U.S. Geological Survey Open-File Report 87-347; U.S. Geological Survey: Reston, Virginia, USA, 1988; pp. 1–23.
32. Bezy, J.; Gutmann, J.; Haxel, G. *A Guide to the Geology of Organ Pipe Cactus National Monument and the Pinacate Biosphere Reserve*; Arizona Geological Survey: Tucson, AZ, USA, 2000; pp. 1–66.
33. Brown, J. *Interpretive Geologic Map of Mt. Ajo Quadrangle, Organ Pipe Cactus National Monument, Arizona*; U.S. Geological Survey Open-File Report 92-23; U.S. Geological Survey: Reston, Virginia, USA, 1992; pp. 1–15.

34. Carruth, R. *Hydrogeology of the Quitobaquito Springs and La Abra Plain area, Organ Pipe Cactus National Monument, Arizona, and Sonora Mexico*; Water-Resources Investigations Report 95-4295; U.S. Geological Survey: Reston, Virginia, USA, 1996; pp. 1–23.
35. Servicio Geológico Mexicano—Cartas Geológicas. Available online: [https://mapserver.sgm.gob.mx/Cartas\\_Online/geologia/168\\_H12-A24\\_GM.pdf](https://mapserver.sgm.gob.mx/Cartas_Online/geologia/168_H12-A24_GM.pdf) (accessed on 25 August 2017).
36. Anderson, T.; Freethy, G.T. *Geohydrology and Water Resources of Alluvial Basins in South-Central Arizona and Parts of Adjacent States*; U.S. Geological Survey Open File Report 89-378; U.S. Geological Survey: Reston, Virginia, USA, 1990; pp. 1–99.
37. Trainer, F. Plutonic and metamorphic rocks. In *The Geology of North America*; Back, W., Rosenshein, J., Seaber, P., Eds.; Geological Society of America: Boulder, CO, USA, 1988; Volume O-2, pp. 367–380.
38. Woloshun, C. Temperature as an Indicator of Flow in Fractured Rock NEAR Oracle, Arizona. Master's Thesis, University of Arizona, Tucson, AZ, USA, 1989.
39. Markovich, K.H.; Manning, A.H.; Condon, L.E.; McIntosh, J.C. Mountain-Block Recharge: A Review of Current Understanding. *Water Resour. Res.* **2019**, *55*, 8278–8304, doi:10.1029/2019WR025676.
40. Robertson, F.N. *Geochemistry of Groundwater in Alluvial Basins of Arizona and Adjacent Parts of Nevada, New Mexico, and California*; Professional Paper 1406-C; U.S. Geological Survey: Reston, Virginia, USA, 1991; pp. 1–91.
41. Baillie, M.N.; Hogan, J.F.; Ekwurzel, B.; Wahi, A.K.; Eastoe, C.J. Quantifying water sources to a semiarid riparian ecosystem, San Pedro River, Arizona. *J. Geophys. Res. (Biogeosci.)* **2007**, *112*, G03S02, doi:10.1029/2006JG000263.
42. National Water Quality Monitoring Council—Water Quality Portal. Available online: <https://www.waterqualitydata.us> (accessed on 18 December 2017).
43. Gieskes, J.; Rogers, W. Alkalinity determinations in interstitial waters of marine sediments. *J. Sediment. Res.* **1973**, *43*, 272–277, doi:10.1306/74D72743-2B21-11D7-8648000102C1865D.
44. Parkhurst, D.; Appelo, C. *User's Guide to PHREEQC (Version 2)—A Computer Program for Speciation, Batch-Reaction, One-Dimensional Transport, and Inverse Geochemical Calculations*; Water-Resources Investigations Report 99-4259; U.S. Geological Survey: Reston, Virginia, USA, 1999; pp. 1–312.
45. Welker, J. ENSO effects on the isotopic ( $\delta^{18}\text{O}$ ,  $\delta^2\text{H}$  and d-excess) of precipitation across the US using a high-density, long-term network (USNIP). *Rapid Comm. Mass Spec.* **2012**, *17*, 1655–1660, doi:10.1002/rcm.6298.
46. Zamora, H.A.; Wilder, T.W.; Eastoe, C.J.; McIntosh, J.C.; Welker, J.; Flessa, K.W. Evaluation of Groundwater Sources, Flow Paths, and Residence Time of the Gran Desierto Pozos, Sonora, Mexico. *Geosciences* **2019**, *9*, 378, doi:10.3390/geosciences9090378.
47. Craig, H. Isotopic variations in meteoric waters. *Science* **1961**, *133*, 213–224, doi:10.1126/science.133.3465.1702.
48. Colleen, F. (National Park Service, Tucson, AZ, USA). Personal communication, 2017.
49. Towne, D. *Ambient Groundwater Quality of the Western Mexican Drainage: A 2016–2017 Baseline Study*; ADEQ Open File Report 17-02; ADEQ Arizona Department of Environmental Quality: Phoenix, AZ, USA, 2018; pp. 1–52.
50. Gu, A.; Gray, F.; Eastoe, C.; Norman, L.; Duarte, O.; Long, A. Tracing ground water input to base flow using sulfate (S, O) isotopes. *Ground Water* **2008**, *46*, 502–509, doi:10.1111/j.1745-6584.2008.00437.x.
51. Eastoe, C.; Hess, G.; Mahieux, S. Identifying recharge from tropical cyclonic storms, Baja California Sur, Mexico. *Ground Water* **2014**, *53*, 133–138, doi:10.1111/gwat.12183.
52. Jasechko, S.; Lechler, A.; Pausata, F.; Fawcett, P.; Gleeson, D. Late-glacial to late-Holocene shifts in global precipitation. *Clim. Past* **2015**, *11*, 1375–1393, doi:10.5194/cp-11-1375-2015.
53. Wagner, J.; Cole, J.; Beck, J.; Patchett, P.; Henderson, G.; Barnett, H. Moisture variability in the southwest United States linked to abrupt glacial climate change. *Nat. Geosci.* **2010**, *3*, 110–113, doi:10.1038/ngeo707.
54. Van Devender, T.; Martin, P.; Thompson, R.; Cole, K.; Jull, A.; Long, A.; Toolin, L.J.; Donahue, D.J. Fossil packrat middens and the tandem accelerator mass spectrometer. *Nature* **1985**, *317*, 610–613, doi:10.1038/317610a0.
55. Van Devender, T. Late Quaternary Vegetation and Climate of the Sonoran Desert, United States and Mexico. In *Packrat Middens: The Last 40,000 Years of Biotic Change*; Betancourt, J., Van Devender, T., Martin, P., Eds.; University of Arizona Press: Tucson, AZ, USA, 1990; pp. 134–165.

56. Stute, M.; Schlosser, P.; Clark, J.F.; Broecker, W.S. Paleotemperatures in the Southwestern United States Derived from Noble Gases in Ground Water. *Science* **1992**, *256*, 1000–1003, doi:10.1126/science.256.5059.1000.
57. Tierney, J.E.; Zhu, J.; King, J.; Malevich, S.B.; Hakim, G.J.; Poulsen, C.J. Glacial cooling and climate sensitivity revisited. *Nature* **2020**, *584*, 569–573, doi:10.1038/s41586-020-2617-x.
58. Meixner, T.; Manning, A.H.; Stonestrom, D.A.; Allen, D.M.; Ajami, H.; Blasch, K.W.; Brookfield, A.E.; Castro, C.L.; Clark, J.F.; Gochis, D.J.; et al. Implications of projected climate change for groundwater recharge in the western United States. *J. Hydrol.* **2016**, *534*, 124–138, doi:10.1016/j.jhydrol.2015.12.027.

**Publisher's Note:** MDPI stays neutral with regard to jurisdictional claims in published maps and institutional affiliations.



© 2020 by the authors. Licensee MDPI, Basel, Switzerland. This article is an open access article distributed under the terms and conditions of the Creative Commons Attribution (CC BY) license (<http://creativecommons.org/licenses/by/4.0/>).